Environment Dependent Coherence of a Short DNA Charge Transfer System

Heeyoung Kim, Myeongwon Lee, and Eunji Sim*

*Department of Chemistry, Yonsei University, Seoul 120-749, Korea. *E-mail: esim@yonsei.ac.kr*

Relationship between charge transfer mechanism and quantum coherence has been investigated using a real-time quantum dynamics approach. In the on-the-fly filtered propagator functional path integral simulation, by separating paths that belong to different mechanisms and by integrating contributions of correspondingly sorted paths, it was possible to accurately obtain quantitative contribution of different transport mechanisms. For a 5'-GAGGG-3' DNA sequence, we analyze charge transfer processes quantitatively such that the governing mechanism alters from coherent to incoherent charge transfer with respect to the friction strength arising from dissipative environments. Although the short DNA sequence requires substantially strong dissipation for completely incoherent hopping transfer mechanism, even a weak system-environment interaction markedly destroys the coherence within the quantum mechanical system and the charge transfer dynamics becomes incoherent to some degree. Based on the forward-backward path deviation analysis, the coherence variation depending on the environment is investigated numerically.

Key Words : Coherence, Charge transfer, DNA, Path integral, Reorganization energy

Introduction

In recent years, bridge-mediated charge transfer (CT) phenomena in DNA sequences have been a topic of tremendous interest. Understanding the CT is essential for the elucidation of the repair process of DNA oxidative damage and for the development of DNA based nanoelectronics and biosensor devices.[1-5]

In general, a short-range CT in DNA has been considered as either of the two controversial mechanisms: G-hopping or A-hopping. In the G-hopping mechanism, it has been suggested that charges are localized on GC base pairs and transfer to distant GC base pairs by coherent superexchange CT through bridging AT (adenine:thymine) base pairs without ever residing on the AT base pairs.[6-9] On the other hand, the A-hopping mechanism proposes that there be a noticeable contribution from incoherent hopping transport, either as a polaron-like hopping or as a true intermediate.[10-13] In particular, the latter has been supported by recent experiments, in which quantitative assessment of the distance dependence of CT efficiency has been shown to be incompatible to that of the exclusively G-hopping mechanism.[11] Using the path integral simulations, we have also found that both incoherent hopping and partially coherent hopping pathways contribute to the charge transport within closely stacked nucleobases within a short 5'-GAGGG-3' sequence.[14] In addition, it was found that the transport dynamics of a system embedded in a dissipative medium is greatly influenced by the fluctuation of the environment, such as phosphate backbone and solvent, owing to the decoherence arising from the frictional interaction between the system and environment.

The mechanism or the dynamics of the CT results from a complex interplay of system structure and the environmental influence. The structure of the DNA CT system denotes the sequence, energy relation and coupling strength between participating electronic states. In general, a quantum mechanical system in vacuum is coherent, while the coherence of the system embedded in a condensed medium is destroyed due to the decoherence arising from the dissipation of a thermal bath. In other words, the system exhibits coherent dynamics in the absence of the bath while incoherent dynamics of the CT become dominant depending on the bath friction strength. Although qualitative characteristics of the influence of the bath dissipation relevant to the transport dynamics have been widely explored and understood, the investigation still lacks quantitative analyses. In particular, in order to understand DNA CT dynamics, quantitative investigation into the coherence variation owing to environments needs to be performed.

In this article, we define and analyze the degree of coherency for studying the influences of environmental decoherence on the CT mechanism. The article is organized as follows: the on-the-fly filtered propagator functional path integral (OFPF-PI) formalism is discussed in section 2 and, in section 3, time evolution of the charge population of a short DNA sequence and the diabatic potential surfaces are discussed at various reorganization energies. The degree of coherency is also characterized in terms of the pair of trajectories that significantly contribute to the transport process. Concluding remarks appear in section 4.

Methodology

CT in 5'-GAGGG-3' DNA double helix is considered as employing a donor(GC base pair)-bridge(AT base pair)-acceptor(triple GC base pair) triad model. Upon injecting charges into the donor state, charges migrate between the D-B-A electronic states under the influence of the surrounding that consists of a phosphate backbone and solvent. The total Hamiltonian is written as

$$H = H_s(s) + H_b(\mathbf{x}) + H_{int}(s,\mathbf{x}) \tag{1}$$

Within the tight-binding system-bath Hamiltonian model, the system Hamiltonian H_s has a matrix representation in terms of three diabatic oxidized electronic states. The bare bath Hamiltonian H_b is composed of an almost infinite number of harmonic oscillator modes and weak bilinear interaction between the system and the bath is assumed within the linear response limit.

Relaxation of the charge population on donor, bridge, and acceptor oxidized electronic states in time is obtained from the reduced density matrix of the system defined as

$$\tilde{\rho}(t) = Tr_b[e^{-iHt/\hbar}\rho(0)e^{iHt/\hbar}] \tag{2}$$

where $\rho(0)$ is the initial density matrix of the system and bath that are separable at thermal equilibrium. The trace with respect to all bath degrees of freedom is denoted as Tr_b. Following Feynman and Vernon's influence functional path integral approach, Eq. (2) can be rewritten as a product of the bare system dynamics in the absence of the bath and the influence functional that describes the environmental effect on the system dynamics:

$$\tilde{\rho}(t) = \sum_i^{L_{tot}} \mathbf{S}(\Gamma_i^{(N)}; \Delta t) \cdot \mathbf{F}(\Gamma_i^{(N)}; \Delta t) \tag{3}$$

where $\Gamma_i^{(N)} \equiv \{(s_0^{\mp})_i, (s_1^{\pm})_i, ..., (s_{N-1}^{\pm})_i, (s_N^{\pm})_i\}$ denotes the ith trajectory, which spans from time 0 to t (forward-direction) and from t to 0 (backward direction), discretized into N time steps, $\Delta t = t/N$. The summation includes all possible paths connecting D-B-A electronic states leading to $L_{tot} = 3^{2N}$. S represents the system propagator that includes the initial system density matrix and one-dimensional forward and backward bare system short-time propagators. On the other hand, **F** is the influence functional with memory that arises from the system-environment interaction. The memory, however, is often finite in time owing to the interference between bath modes.

The OFPF-PI approach effectively treats the non-Markovian dynamics of a single-time reduced density matrix as a pseudo-Markovian dynamics of a multi-time augmented reduced density matrix. Assuming the bath memory spans N_τ time steps and by implementing on-the-fly filtering of the significant path segments, Eq. (3) is rewritten as

$$\tilde{\rho}(t) = \sum_{w_i > \theta} \mathbf{S}(\Gamma_i; t) \cdot \mathbf{F}(\Gamma_i; t), \quad N \leq N_\tau \tag{4}$$

$$\tilde{\rho}(t) \approx \sum_{w_i > \theta} \mathbf{S}(\Gamma_i'; t) \cdot \mathbf{F}(\Gamma_i'; t), \quad N > N_\tau \tag{5}$$

where the summation includes only the paths with the weight, $w_i = |\mathbf{S}(\Gamma_i; t) \cdot \mathbf{F}(\Gamma_i; t)|$, bigger than the cutoff θ. Notice the truncated trajectory in Eq. (5), $\Gamma_i' \equiv \{(s_{N-N_\tau}^{\mp})_i, (s_{N-N_\tau-1}^{\pm})_i, ..., (s_{N-1}^{\pm})_i, (s_N^{\pm})_i\}$, in which the dynamics between time points that are separated by more than N_τ time steps are ignored. The OFPF-PI method is practical and useful in exploring quantum transport phenomena since it allows quantitative analysis on the dynamic contribution of an individual pathway. Details of the OFPF-PI approach can be found elsewhere.[15,16]

Results and Discussion

Consider a system that consists of a GC single pair (donor) and a GC triple pair (acceptor) separated by an AT base pair (bridge). Based on the tight-binding model, localized hole states in nucleobase pairs are represented by corresponding oxidation potentials. By taking relative oxidation potential energy differences, the acceptor state energy is taken to be 0.096 eV lower while the bridge state energy is 0.47 eV higher than the donor state energy.[17,18] The donor-bridge and bridge-acceptor electronic coupling constants are chosen to be sequence independent as $V_{GA} = V_{AG} = 0.025$ eV.[19,20] Each electronic state is assumed to interact only with its nearest-neighbors and the system is initially in the donor state at room temperature. Aforementioned model parameters to describe necleobase oxidation are relatively well-known compared to the solvent properties that affect the CT dynamics, although value of the reorganization energy that represents the environmental influence is still in debate.

The reorganization energy is the free energy required to deform nuclear coordinates of a molecule as well as the environment from the equilibrium configuration of the donor state to that of the bridge and the product state. Dissipation arising from the environment is often represented by a spectral density.

$$J(\omega) = \frac{\pi}{2} \sum_j \frac{c_j^2}{m_j \omega_j} \delta(\omega - \omega_j) \tag{6}$$

In this work, we chose the Debye model that has the form,

$$J(\omega) = \frac{j_d \omega}{\omega^2 + \omega_d^2} \tag{7}$$

where ω_d denotes the characteristic Debye frequency and j_d the friction strength. Reorganization energy, λ, owing to the differences in donor and acceptor molecular geometries and to the changes of nuclear coordinates of the surrounding medium, is evaluated from the spectral density as

$$\lambda = \frac{R_{DA}^2}{\pi} \int_0^\infty d\omega \frac{J(\omega)}{\omega} \tag{8}$$

with R_{DA} being the distance between the donor and the acceptor.

A. Diabatic Surface Crossings. Figures 1(a) through 5(a) show diabatic potential surfaces at various reorganization energies ranging 0.008-2.37 eV. Notice positions of the potential surface crossings with respect to the reorganization energy. Time-evolution of the three diagonal elements of the reduced density matrix corresponds to the charge density relaxation at individual electronic states and is also shown in Figures 1(b) through 5(b). Decay of the charge density at the donor over time represents the CT to the bridge and acceptor while a rise of the acceptor population describes the charge accumulation due to charge trapping on the energetically favorable GC triple pair.

In order to explore the transfer mechanism both qualitatively and quantitatively, decomposition of the density matrix
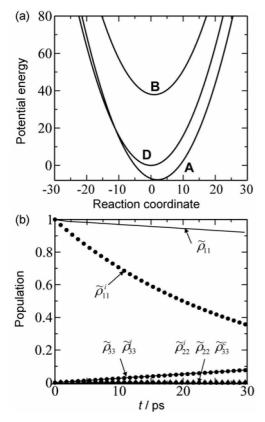
Figure 1. (a) Schematic diagram of diabatic potential energy surfaces (D for donor, B for bridge, and A for acceptor) and (b) time-evolution of the charge accumulation on the three electronic states coupled to the Debye spectral density with the reorganization energy $\lambda = 0.008$ eV. In (b), solid lines correspond to the diagonal elements of the full reduced density matrix for which all possible paths are taken into account while circles correspond to the partial density matrix of the incoherent hopping mechanism. The coherent superexchange contribution to the acceptor charge accumulation is also plotted as triangles but negligible.

in terms of partial terms corresponding to possible mechanisms should be performed. Unlike the wavefunction propagation approaches, each pathway in path integration of the reduced density matrix is uncorrelated with others allowing independent computation of the path contribution to the density matrix. Therefore, the reduced density matrix of the system can be written as the sum of partial density matrices of four mechanisms such that

$$\tilde{\rho}(t) = \tilde{\rho}^i(t) + \tilde{\rho}^c(t) - \tilde{\rho}^p(t) + \tilde{\rho}^s(t), \qquad (9)$$

where superscript i stands for incoherent hopping, c for coherent superexchange, p for partially coherent hopping, and s for static pathways. Partially coherent hopping pathways are plausible such that, within a single path segment, charges hop between donor and bridge and from donor to acceptor. In addition, some pathways have static characteristics for which charges may not transfer from their initial state without any contribution to CT. From Figures 1(b) through 5(b), it is clearly shown that both incoherent hopping and partially coherent hopping pathways contribute to the charge transport of 5'-GAGGG-3'. No charge accumu-
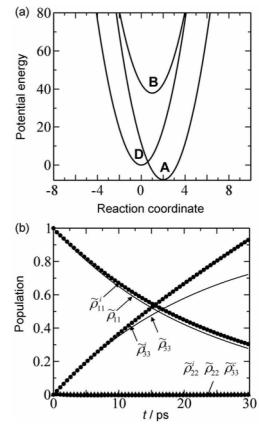

Figure 2. Same as Fig. 1 with the reorganization energy $\lambda = 0.25$ eV.

lation on the bridge is observed due to a rapid transfer of charges from energetically unfavorable bridge to the favorable acceptor. Furthermore, a coherent superexchange pathway contributes negligibly to the rise of the acceptor population, supporting the interplay between incoherent and partially coherent CT mechanisms.

With an increase of the bath friction, potential surface crossings between the donor and acceptor move through activationless region, eventually to the normal region. The activation energy decreases with the reorganization energy until the position of the curve crossing reaches the activationless regime. As the curve crossing position passes through the activationless region, the activation energy increases following the reorganization energy. For this reason, we observe the Kramer's turnover as a function of the bath friction strengths in CT rate constants.

Although the overall CT is moving toward the incoherent hopping limit, it was observed in Figure 3(b) that the net CT contribution from the donor state to the acceptor through incoherent hopping pathways seems to decrease. While the activation is still quite large, the potential crossing between the donor and bridge and the bridge and acceptor requires significantly smaller amount of the activation energy compared to Figures 1(a) and 2(b). With $\lambda = 1.11$ eV, the position of the donor-acceptor diabatic surface crossing is still lower in energy than that of the donor-bridge activation energy. Nevertheless, the overall contribution of the incoherent pathways steadily increases and the CT mechanism becomes
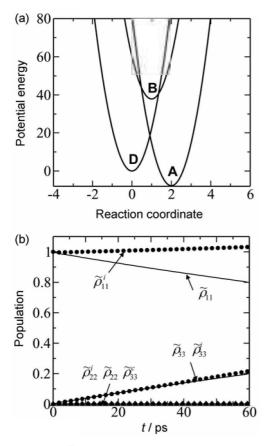
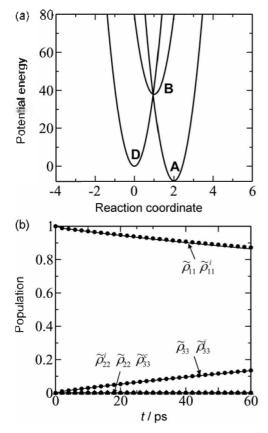**Figure 3.** Same as Fig. 1 with the reorganization energy $\lambda = 1.11$ eV.

Figure 4. Same as Fig. 1 with the reorganization energy $\lambda = 2.05$ eV.
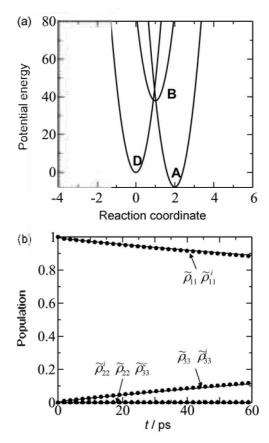

Figure 5. Same as Fig. 1 with the reorganization energy $\lambda = 2.37$ eV.

completely incoherent as the three potential surfaces cross at a single position. Figure 4(b) clearly presents that the CT mechanism has reached complete incoherence due to the strong dissipation of the thermal bath and that the transfer population through the incoherent hopping pathways coincides with the full density matrix. Once the system configuration reaches the incoherent limit, the CT mechanism is no longer influenced by the reorganization energy as depicted in Figures 4 and 5.

The coherence within the states is also well described by the oscillation in the population relaxation. Figures 6(a) and 6(b) show short-time decays of the donor population with the reorganization energy at $\lambda = 0.0016$ eV and $\lambda = 2.37$ eV, respectively. With small friction, the CT dynamics is substantially coherent while the donor and acceptor states exhibit coherent oscillations in their population relaxation as shown in Figure 6(a). The acceptor state population change, which is not shown here, also oscillates correspondingly with that of the donor state. On the other hand, as the friction strength becomes larger, the coherence is destroyed and the oscillation in the population relaxation is significantly suppressed. In Figure 6(b) with strong friction, an oscillatory relaxation profile is no longer observed. The initial dip in the donor population is due to the rapid CT to the bridge state through incoherent hopping pathways.

B. Degree of Coherence. In Eqs. (4) and (5), the influence functional **F** is complex, thus it is possible to split it into real
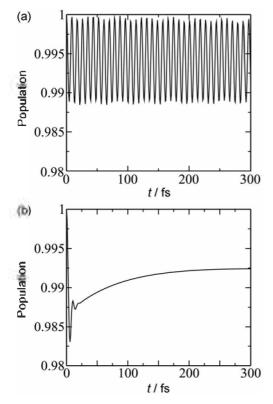
Figure 6. Decay of the donor population in short time scale with the reorganization energy at (a) $\lambda = 0.0016$ eV and (b) $\lambda = 2.05$ eV.

Figure 7. Time average of forward and backward path difference and its standard deviation with respect to the reorganization energy.

Figure 8. Charge transfer rate constants as a function of the reorganization energy.

and imaginary parts such that[16]

$$\mathbf{F} = \exp\left(-\sum_{k=0}^{N} \sum_{k'=0}^{k} \frac{\varepsilon_{kk'}}{\hbar} \Delta_k \Delta_{k'}\right)$$

$$\times \exp\left(-i \sum_{k=0}^{N} \sum_{k'=0}^{k} \frac{\varphi_{kk'}}{\hbar} \Delta_k [\Delta_{k'} - 2\bar{s}_{k'}^-]\right) \quad (10)$$

where real-valued $\varepsilon_{kk'}$ and $\varphi_{kk'}$ denotes influence coefficients. $\Delta_k = \Delta(k\Delta t) = \bar{s}_k^- - \bar{s}_k^-$ represents the forward-backward path distance at time $k\Delta t$. According to Eq. (8), the magnitude of the influence functional is large if $\Delta_k \Delta_{k'} \leq 0$ for all combinations of k and k'. In particular, classically allowed paths correspond to $\Delta_k = 0$ at any k.

In Eq. (10), $\Delta(t) = s^-(t) - s^-(t)$ denotes difference between the forward and backward paths at a given time. By taking time average of $\Delta(t)$ and evaluating its standard deviation, $\langle|\Delta|\rangle - \sigma$ indicates the distance between strongly coherent states. In Figure 7, the time average of the absolute forward and backward path deviation, $\langle|\Delta|\rangle$, is presented along with its standard deviation, σ, as a function of the reorganization energy.[16] Both the average and the standard deviation decrease with respect to the friction strength. In our tight-binding model, the distance between the nearest-neighbor states was set to be equal to unit distance. For the 5'-GAGGG-3' short DNA sequence in Figure 7, $\langle|\Delta|\rangle + \sigma > 1$ in the weak friction regime suggests that the difference between the forward and backward quantum mechanically contributing paths extend up to the next-nearest-neighbor
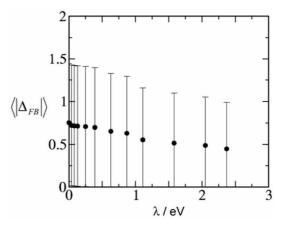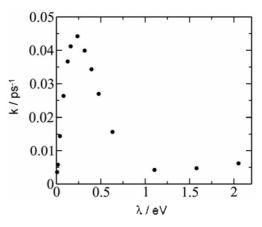
states. In other words, the coherence between the donor and acceptor state is markedly strong. It also confirms that both incoherent hopping and partially coherent hopping pathways contribute to CT processes.[14] As the reorganization energy increases, $\langle|\Delta|\rangle + \sigma$ is decreased. In the strong friction regime, $\langle|\Delta|\rangle + \sigma \leq 1$ such that difference between the forward and backward quantum mechanical paths spans no further than $\langle|\Delta|\rangle + \sigma \leq 1$ verifying that the coherence between states is destroyed owing to the strong bath friction and that significantly contributing pathways resemble classical counterparts.

Finally, Figure 8 shows the CT rate constants as a function of the reorganization energy. The most efficient CT was achieved at $\lambda = 0.25$ eV in which the dynamics is not governed by a single CT mechanism but rather by the interplay between incoherent and coherent migrations. It is interesting to note that the activation energy is so large that the overall CT is inefficient as the configuration reaches the incoherent hopping limit. With femto-second resolution, Wan et al. observed time constants of 5 ps and 75 ps in case of an ethidium modified 3'-ETGG-5' DNA sequence.[21] Figure 8 also shows time constants between 16 and 200 ps that agree qualitatively with experimental observations.

Concluding Remarks

In this article, we investigated the charge transport mechanism in a short DNA sequence using the OFPF-PI method. By separating paths that belong to different mechanisms and by independently integrating contributions of each path, it was possible to determine the role of different pathways to the overall CT process. It has been well known that the reorganization energy due to a dissipative medium affects the coherence of the system and eventually CT dynamics. As far as we know, the change of the CT mechanism as well as the degree of coherency with respect to the reorganization energy has not been presented on a quantitative basis. In this article, we considered a 5'-GAGGG-3' DNA sequence embedded in a condensed medium with various strengths of dissipation to investigate the relative contribution of the CT mechanisms. The CT process is dominated by coherent migrations in the limit of weak bath friction, while it becomes incoherent hopping dominated in the strong friction limit. It was found that, although the short DNA sequence requires substantially strong dissipation for completely incoherent hopping mechanism, even a tiny reorganization energy significantly destroys the coherence within the bare system such that the incoherent hopping transport cannot be ignored. In general, the incoherent hopping mechanism is required to achieve the most efficient CT within molecular wire-type CT systems. For the short DNA sequence considered in this article, we have observed that the most efficient CT was achieved not by the incoherent hopping pathways but by the interplay between the incoherent hopping and superexchange migrations. Although the implication of the finding in the long-range CT systems should be examined in further studies, it would be interesting to note that the interplay between coherent and incoherent migrations may provide the most efficient dynamics in a given CT system.

References

1. Porath, D.; Bezryadin, A.; De Vries, S.; Dekker, C. *Nature* **2000**, *403*, 635.
2. Cai, L.; Tabata, H.; Kawai, T. *Appl. Phys. Lett.* **2000**, *77*, 3105.
3. Boon, E. M.; Ceres, D. M.; Drummond, T. G.; Hill, M. G.; Barton, J. K. *Nat. Biotechnol.* **2000**, *18*, 1096.
4. Dandliker, P. J.; Holmlin, R. E.; Barton, J. K. *Science* **1997**, *275*, 1465.
5. Kelley, S. O.; Barton, J. K. *Science* **1999**, *283*, 375.
6. Bixon, M.; Giese, B.; Wessely, R.; Langenbacher, T.; Michel-Beyerle, M. E.; Jortner, J. *Proc. Natl. Acad. Sci. U.S.A.* **1999**, *96*, 11713.
7. Berlin, Y. A.; Burin, A. L.; Ratner, M. A. *Chem. Phys.* **2002**, *275*, 61.
8. Brozema, F. C.; Berlin, Y. A.; Siebbeles, L. D. *J. Am. Chem. Soc.* **2000**, *122*, 10903.
9. Voityuk, A. A.; Rösch, N.; Bixon, M.; Jortner, J. *J. Phys. Chem. B* **2000**, *104*, 9740.
10. Henderson, P. T.; Jones, D.; Hampikian, G.; Kan, Y.; Schuster, G. B. *Proc. Natl. Acad. Sci. U.S.A.* **1999**, *96*, 8353.
11. Sartor, V.; Boone, E.; Schuster, G. B. *J. Phys. Chem. B* **2001**, *105*, 11057.
12. Conwell, E. M.; Rakhmanova, S. V. *Proc. Natl. Acad. Sci. U.S.A.* **2000**, *97*, 4556.
13. Zhang, H.; Li, X.-Q.; Hang, P.; Yu, X. Y.; Yan, Y. *J. Chem. Phys.* **2002**, *117*, 4578.
14. Kim, H.; Sim, E. *J. Phys. Chem. B* **2006**, *110*, 631.
15. Sim, E. *J. Chem. Phys.* **2001**, *115*, 4450.
16. Sim, E.; Kim, H. *J. Phys. Chem. B* **2006**, *110*, 13642.
17. Voityuk, A.; Jortner, J.; Bixon, M.; Rösch, N. *Chem. Phys. Lett.* **2000**, *324*, 430.
18. Bixon, M.; Jortner, J. *Chem. Phys.* **2002**, *281*, 393.
19. Troisi, A.; Orlandi, G. *Chem. Phys. Lett.* **2001**, *344*, 509.
20. Renger, T.; Marcus, R. A. *J. Phys. Chem. A* **2003**, *107*, 8404.
21. Wan, C.; Fiebig, T.; Kelley, S. O.; Treadway, C. R.; Barton, J. K.; Zewail, A. H. *Proc. Natl. Acad. Sci. U.S.A.* **1999**, *96*, 6014.